Effects of fluorine incorporation into β-Ga_2O_3

Jiangcheng Yang, Chaker Fares, F. Ren, Ribhu Sharma, Erin Patrick, Mark E. Law, S. J. Pearton, and Akito Kuramata

Citation: Journal of Applied Physics **123**, 165706 (2018); doi: 10.1063/1.5031001
View online: https://doi.org/10.1063/1.5031001
View Table of Contents: http://aip.scitation.org/toc/jap/123/16
Published by the American Institute of Physics

Effects of fluorine incorporation into β-Ga_2O_3

Jiangcheng Yang,[1] Chaker Fares,[1] F. Ren,[1] Ribhu Sharma,[2] Erin Patrick,[3] Mark E. Law,[3] S. J. Pearton,[2] and Akito Kuramata[4]
[1]*Department of Chemical Engineering, University of Florida, Gainesville, Florida 32611, USA*
[2]*Department of Materials Science and Engineering, University of Florida, Gainesville, Florida 32611, USA*
[3]*Department of Electrical Engineering, University of Florida, Gainesville, Florida 32611, USA*
[4]*Tamura Corporation and Novel Crystal Technology, Inc., Sayama, Saitama 350-1328, Japan*

(Received 27 March 2018; accepted 12 April 2018; published online 30 April 2018)

β-Ga_2O_3 rectifiers fabricated on lightly doped epitaxial layers on bulk substrates were exposed to CF_4 plasmas. This produced a significant decrease in Schottky barrier height relative to unexposed control diodes (0.68 eV compared to 1.22 eV) and degradation in ideality factor (2.95 versus 1.01 for the control diodes). High levels of F ($>10^{22}$ cm^{-3}) were detected in the near-surface region by Secondary Ion Mass Spectrometry. The diffusion of fluorine into the Ga_2O_3 was thermally activated with an activation energy of 1.24 eV. Subsequent annealing in the range 350–400 °C brought recovery of the diode characteristics and an increase in barrier height to a value larger than in the unexposed control diodes (1.36 eV). Approximately 70% of the initial F was removed from the Ga_2O_3 by 400 °C, with the surface outgas rate also being thermally activated with an activation energy of 1.23 eV. Very good fits to the experimental data were obtained by integrating physics of the outdiffusion mechanisms into the Florida Object Oriented Process Simulator code and assuming that the outgas rate from the surface was mediated through fluorine molecule formation. The fluorine molecule forward reaction rate had an activation energy of 1.24 eV, while the reversal rate of this reaction had an activation energy of 0.34 eV. The net carrier density in the drift region of the rectifiers decreased after CF_4 exposure and annealing at 400 °C. The data are consistent with a model in which near-surface plasma-induced damage creates degraded Schottky barrier characteristics, but as the samples are annealed, this damage is removed, leaving the compensation effect of Si donors by F^- ions. The barrier lowering and then enhancement are due to the interplay between surface defects and the chemical effects of the fluorine. *Published by AIP Publishing.*
https://doi.org/10.1063/1.5031001

INTRODUCTION

The role of fluorine in compound semiconductors has been of interest since the initial observations of partially reversible changes in the two dimensional electron gas (2DEG) concentration (N_S) in AlInAs/InGaAs modulation-doped structures upon thermal annealing at low temperatures (280 °C).[1–4] A number of experiments involving Hall measurements of SiN_x-passivated versus capless samples, together with chemical profiling of impurities in the near-surface region, established that the recovery of N_S was associated with the outdiffusion of fluorine atoms from the Si-doped n-type InAlAs layer.[2,3] The thermally activated diffusion of fluorine into the Si-doped AlInAs layer was found to be the main cause of the reduction in carrier density, and subsequent annealing could effectively recover the original N_S values.[1–4] This effect has been used to control the threshold voltage in both AlInAs and AlGaN/GaN High Electron Mobility Transistors (HEMTs) through compensating Si donors with the negatively charged F ions.[5–8] The fluorine can be incorporated during exposure to wet chemical solutions such as HF, by direct implantation of low energy fluorine ions or by immersion in a fluorine-containing plasma. The fluorine atoms are strongly electronegative and become negatively charged, effectively raising the potential in the AlGaN or AlInAs barrier and therefore in the 2DEG channel. As a result, the HEMT threshold voltage can be shifted to positive values, and enhancement mode devices can be fabricated.

Recent results have postulated that similar effects may occur in Ga_2O_3 rectifiers, in which larger-than-expected effective barrier heights of 1.46 eV for Pt (compared to 1.16 eV in reference samples) were obtained for samples exposed to hydrofluoric acid prior to metal deposition.[9] The results were consistent with F atoms acting as negative ions and compensating the ionized Si donors in the Ga_2O_3 to form neutral complexes, leading to additional surface depletion.[9] However, no direct confirmation of the presence of fluorine was made, nor any details of the thermal stability of the effect. Since Ga_2O_3 is attracting significant recent attention for use in high power electronics and solar blind UV photodetectors,[10–26] there is a need to more fully understand the effects of unintentionally incorporated impurities such as fluorine and hydrogen, both of which may have strong effects on the doping in the near-surface region.[27–29] There are few effective wet etchants for Ga_2O_3 and patterning of this material is typically done by dry etching methods.[30–33] This means that post-etch residues are usually removed with acid and solvent solutions and that the Ga_2O_3 surface is additionally exposed to such solutions during patterning of dielectrics.

In this paper, we show that high concentrations of fluorine are incorporated into the near-surface region of Ga_2O_3

during exposure to CF_4 plasmas and that it remains in the material to temperatures beyond 400 °C. We use Schottky rectifier structures to elucidate the mechanisms of barrier lowering and subsequent enhancement during plasma exposure and annealing to remove plasma damage. Our previous plasma damage work showed barrier lowering for such surfaces, as evidenced by the increased forward and reverse leakage in diodes fabricated on those surfaces.[32,33] A post-gate annealing at a gate electrode- compatible temperature of 400 °C proved to be effective in recovering the initial plasma-induced damage. Once this damage was annealed, the gate leakage current at reverse bias was decreased by one to two orders of magnitude. This is also consistent with the temperatures at which point defect damage in Ga_2O_3 is observed to anneal out.[34,35] The barrier height was also increased relative to control samples not exposed to fluorine, showing that compensation of Si donors by F^- ions occurs in Ga_2O_3. The dominant mechanisms for the outdiffusion kinetics were extracted from simulations using the Florida Object Oriented Process Simulator (FLOOPS) code.

EXPERIMENTAL

The starting material consisted of vertical structures of epitaxial layers (7 μm final thickness) of lightly Si-doped n-type (5.2×10^{16} cm^{-3}) Ga_2O_3 grown by Hydride Vapor Phase Epitaxy (HVPE) on n^+ bulk, β-phase Sn-doped Ga_2O_3 single crystal wafers (~650 μm thick) with (001) surface orientation (Tamura Corporation, Japan). The source gases used were GaCl and O_2 transported by a N_2 carrier gas. GaCl was generated in the upstream region of the reactor by the reaction between high-purity Ga metal (6N grade) and chlorine (Cl_2) gas at 850 °C. GaCl and O_2 were separately introduced to the downstream region (growth zone) where the β-Ga_2O_3 substrate was placed on a quartz glass susceptor. The growth zone was heated to a temperature between 800 and 1050 °C under a flow of N_2 containing O_2 at a partial pressure of 2.5×10^{-3} atm. The β-Ga_2O_3 layer was subsequently grown by supplying GaCl with an input partial pressure of 5.0×10^{-4} atm with a fixed input VI/III ($2O_2$/GaCl) ratio of 10. The total gas flow rate was 1600 sccm throughout the entire growth process. The substrates were grown by the edge-defined film-fed method. These substrates had carrier concentration of 3.6×10^{18} cm^{-3} as obtained from Hall measurements. The dislocation density from etch pit observation was of the order of 10^3 cm^{-2}, and the x-ray diffraction full-width-half maximum was 137 arc sec. The HVPE layers were treated by chemical mechanical planarization to remove pits, as described previously and the back surface of the substrate was also polished to remove sub-surface damage and enhance Ohmic contact formation.

Diodes were fabricated by depositing full area back Ohmic contacts of Ti/Au (20 nm/80 nm) by E-beam evaporation and annealed in an SSI Solaris 150 rapid thermal annealing (RTA) system at 550 °C for 30 s under nitrogen ambient. A 100 nm of SiNx film was deposited onto the sample surface with a plasma enhanced chemical vapor deposition system at 300 °C using silane and ammonia. Prior to the film deposition, the sample surface was treated with ozone for 10 min to remove any carbon contaminations. The SiN_x contact windows were patterned with standard lithography process and opened with Technics reactive ion etching (RIE) system with CF_4 plasma [150 mTorr (20 Pa), CF_4 flow rate of 30 sccm, and 50 W power]. The sample was then exposed in CF_4 plasma for additional 5 min after the opening of these SiN_x windows. We also made reference samples with no plasma exposure and samples exposed to Ar plasma under the same power and time conditions to simulate the effect of plasma damage, but not chemical effect of fluorine. The front side Schottky contacts were overlapped 5 μm on the SiN_x window opening and formed by standard lift-off of E-beam deposited Ni/Au (20 nm/150 nm). The size of these contacts was 40 μm × 40 μm. The CF_4 exposed samples were diced into pieces and annealed at 350 and 400 °C for 10 min under nitrogen ambient. Figure 1 shows a schematic of the rectifier structure. For the reference sample, the same processing procedures were employed without SiN_x deposition and CF_4 etching. For the Secondary Ion Mass Spectrometry (SIMS) study, four blank samples were exposed to the same CF_4 plasma conditions for 20 min. The annealing process for the three of these four samples was carried out at 300, 400, or 500 °C for 10 min under N_2 ambient.

Current-voltage (I-V) and capacitance-voltage (C-V) characteristics were recorded in air at 25 °C on an Agilent 4145B parameter analyzer. The sweep direction for both was from positive to negative voltages. The fluorine depth profiles were measured in as-exposed and annealed samples using Secondary Ion Mass Spectrometry (SIMS) employing a Cs^+ primary ion beam, while secondary ions formed during the sputtering process were extracted and analyzed using a quadrupole mass spectrometer.[36] Implanted standards were used to get quantification of the fluorine concentrations. The numerical simulation of the fluorine outdiffusion kinetics was carried out using the FLOOPS TCAD simulator.[37,38] This employs finite element discretization methods written in C++ code to solve the coupled, partial differential equations needed for device or process simulation. FLOOPS is unique in that it has its own command-line, scripting language that allows for the easy formulation of analytical models to describe the device physics.[39,40] The Poisson equation, equations for continuity of electrons and holes, and current density comprise the coupled, partial differential equations used by the simulator.

RESULTS AND DISCUSSION

Figure 2 shows the I-V characteristics on linear (top) and log scales (bottom) for the reference and CF_4 plasma

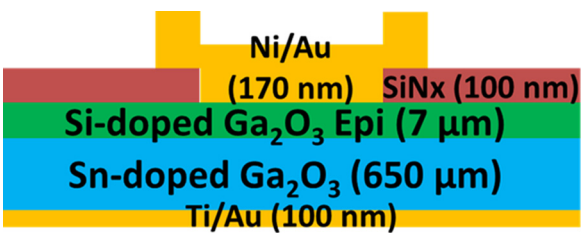

FIG. 1. Schematic of edge terminated, vertical geometry β-Ga_2O_3 Schottky rectifier structure used in these experiments.

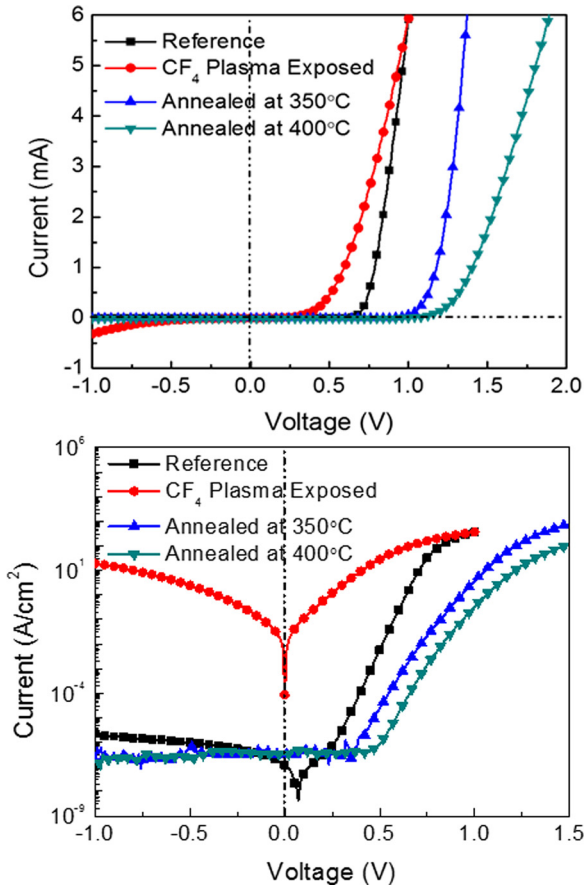

FIG. 2. Simulation of conduction band energy levels (E_c) as a function of distance into the Ga_2O_3 epitaxial layer for various experimental conditions. E_c is referenced to the quasi Fermi level. The barrier height, Φ_b, for each case can be read directly from the graph.

exposed diode samples, as well as those subsequently annealed at 350 or 400 °C with the Schottky contact in place. The effect of the plasma exposure is to increase both the forward and reverse currents, while annealing reverses this trend and leads to lower currents than in the unexposed reference diodes. The ideality factor, n, and Schottky barrier heights, Φ_B, were obtained by fitting the linear region of the I–V curve to the thermionic emission (TE) model, as reported previously.[9] Near-ideal Schottky characteristics with n values of 1.01 were obtained for the reference diodes, with a barrier height of 1.22 eV, consistent with past results. We used the I-V data rather than C-V data because nonlinear doping profiles can affect the latter. Similar data were obtained for the plasma exposed and subsequently annealed diodes and are tabulated in Table I. We also calculated the on-state resistance, R_{ON}. Note that the barrier height is significantly degraded after plasma exposure and then recovers to values larger than in the reference diodes upon subsequent annealing. Simulation of the conduction band energy levels corresponding to the different experimental conditions, shown in Fig. 3, depicts the changes in barrier height. The barrier height lowering also correlated with a large increase in ideality factor in the plasma exposed diodes, consistent with introduction of generation-recombination centers and multiple current transport mechanisms rather than pure thermionic emission. Note that full recovery of the ideality

TABLE I. Diode parameters before and after CF_4 plasma exposure and subsequent annealing at different temperatures, both with and without the Schottky contact in place during the anneal.

Device	Barrier height (eV)	Ideality factor	On-resistance (Ω cm^2)
Reference	1.22	1.01	6.53×10^{-4}
CF_4 treated	0.68	2.95	1.13×10^{-3}
CF_4 + 350 °C anneal with contact	1.24	1.38	2.35×10^{-4}
CF_4 + 400 °C anneal with contact	1.36	1.27	1.35×10^{-3}

factor and on-resistance did not occur by 400 °C, and beyond this, we noted contact degradation due to thermal reaction with the Ga_2O_3, as noted previously.[32,33]

The same trends of deterioration in electrical properties after plasma exposure, followed by recovery after annealing, were observed in the reverse bias characteristics, shown in more detail in the current density-voltage (J-V) data in Fig. 4. The top of the figure shows the data in linear form, while the bottom shows it on a semi-log scale. The reverse breakdown voltage of >100 V was severely degraded by CF_4 plasma exposure to a value of ~5 V. The breakdown voltage showed the onset of recovery after annealing at 350 °C and was again >100 V for 400 °C anneals. The current in reverse biased Ga_2O_3 diodes is generally found to follow thermionic field emission rather than pure thermionic emission because the large barrier heights for most metal contacts favor tunneling through the barrier over thermal emission over this barrier.[11,13,17,18] Both the forward and reverse current characteristics are consistent with plasma-induced damage leading to barrier lowering and introduction of other current transport mechanism; we reported previously for dry etch damage studies in Ga_2O_3. The annealing reduces the density of damage-induced centers to the point where the F^- compensation of Si^+ donors can be observed through the increase in barrier height.

We want to emphasize that reference samples not exposed to fluorine, but exposed to Ar plasmas, annealing at 450 °C was found to essentially restore the values of Φ_B, n,

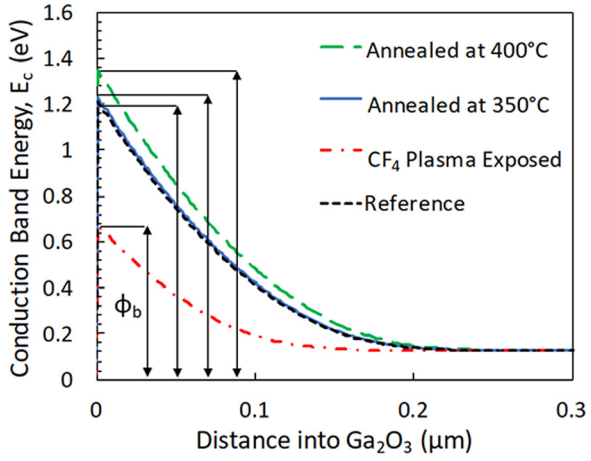

FIG. 3. Current (top) and current density-voltage (bottom) characteristics from rectifiers exposed to CF_4 plasmas prior to Schottky metal deposition and then annealed at 350 or 400 °C with the metal in place.

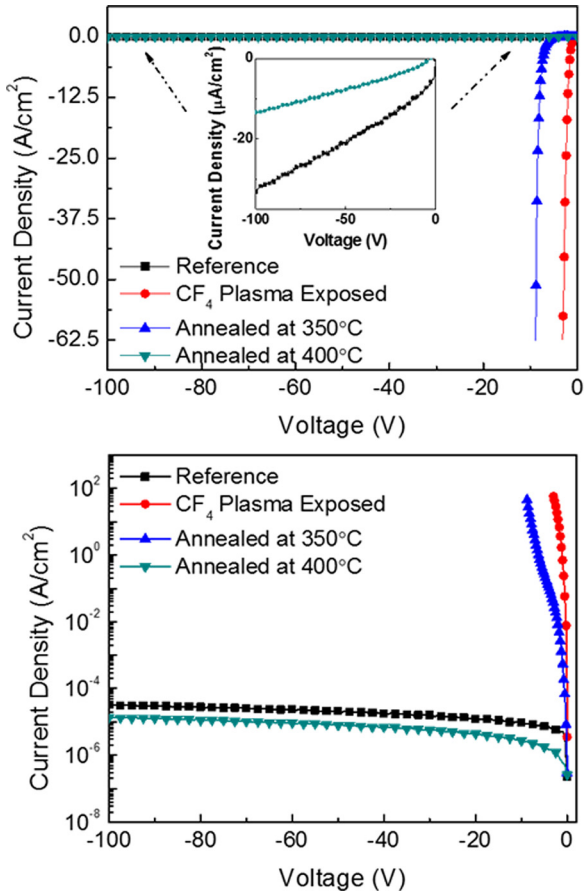

FIG. 4. Reverse current density-voltage characteristics from rectifiers exposed to CF_4 plasmas prior to Schottky metal deposition, and then annealed at 350 or 400 °C with the metal in place shown on a linear (top) or semi-log scale (bottom).

and V_{RB} to their reference (unetched) values on samples metallized after etching and annealing.[33] Thermal annealing at either temperature of metallized diodes degraded their reverse breakdown voltage, showing that Ni/Au is not stable on β-Ga_2O_3 at these temperatures.[33]

Figure 5 shows the rectifier on/off ratio when switching from +1 V forward bias to the reverse voltages shown on the x-axis. The unexposed rectifiers showed on/off ratios of $>10^7$ across the entire voltage range investigated. This was severely degraded by CF_4 plasma exposure, and the measurement is limited in range by the low breakdown voltage in those diodes. This is due to the reduction of rectification ratio as both forward and reverse currents are increased. Annealing at 350 °C again provides a small recovery effect, while annealing at 400 °C restored the on/off ratios to $>10^7$ and is higher than in the control diodes due to the larger barrier height. These results show how the operating characteristics of the rectifiers are degraded by exposure to CF_4 plasmas. We could not anneal the metallized samples at higher temperatures due to the onset of reactions with the Ga_2O_3.

To understand more about the changes resulting from the F incorporation, C-V measurements of these devices with and without CF_4 plasma treatment and subsequent annealing at 400 °C were performed. Figure 6 shows the C^{-2}–V characteristics, which yielded average n-type donor concentrations (N_D) from the slope of the relationship

$$C^{-2} = [2/(e.\varepsilon.\varepsilon_r N_D)] \times (V_{bi} - V - (kT/e))$$

of $5.20 \times 10^{16}\,cm^{-3}$ for the control diodes and $3.94 \times 10^{16}\,cm^{-3}$ for the diodes annealed at 400 °C. In this equation, e is the electronic charge, ε and ε_r are the absolute and relative permittivities, V_{bi} is the built-in voltage, and T the temperature. This reduction in the ionized donor density is consistent with the effect of F^- compensation of Si donors being responsible for the changes in the annealed diodes. Note that the C^{-2}-V plot is slightly curved, indicating a non-uniform doping near the surface. Using the procedures discussed by Ringel *et al.*,[41] the slope is consistent with a near-surface doping of 4.5×10^{16} cm^{-3} and "bulk" doping of 3.1×10^{16} cm^{-3} in the diodes annealed at 400 °C. This does not affect the basic conclusion of a reduction in the net carrier density due to F incorporation. The barrier height determined by this approach was 1.42 eV compared to 1.36 eV. The barrier height determination is complex when factors such as an inhomogeneous distribution of barrier heights, interfacial layers, and series resistance effects may be

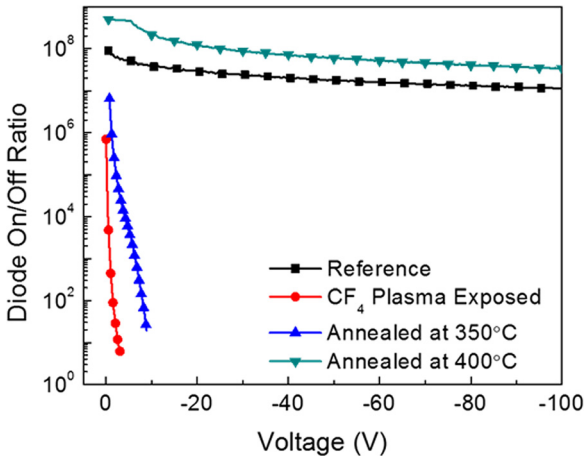

FIG. 5. Diode on/off ratio from rectifiers exposed to CF_4 plasmas prior to Schottky metal deposition, and then annealed at 350 or 400 °C with the metal in place.

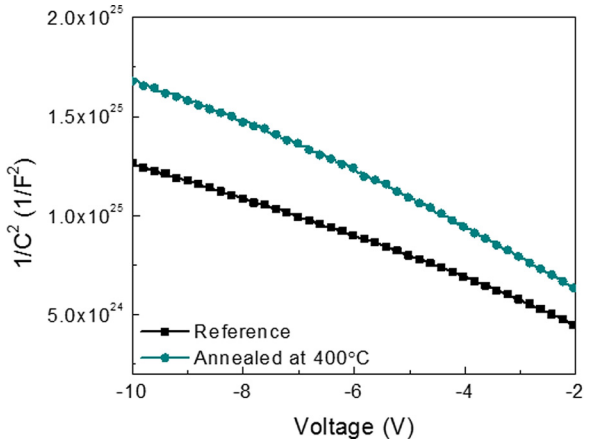

FIG. 6. C^{-2}-V characteristics from a reference diode and one that was exposed to CF_4 plasmas prior to Schottky metal deposition, and then annealed at 400 °C with the metal in place.

present. To allow a consistent comparison of the effects of F, we used the I-V data.

The SIMS profiles of F in Ga_2O_3 exposed to a CF_4 plasma and subsequently annealed in the range 300–500 °C are shown in Fig. 7. This is direct evidence for the incorporation of fluorine in Ga_2O_3 and shows the very high concentration retained (~25% of the original, Fig. 7), even after 500 °C anneals. The SIMS profiles show that F in Ga_2O_3 behaves differently during annealing compared to AlInAs. In the latter case, the F diffuses further into the AlInAs, with a relationship of the form $D = 0.027 \exp(-1.13\,\text{eV/kT})$,[3] where the low activation energy indicates interstitial diffusion. In the case of Ga_2O_3, there is a high concentration, near-surface population, which may be due to molecular fluorine, F_2, since there is no indication that such a high concentration of this impurity is charged. The tail at lower concentration that extends to ~500 Å also out-diffuses and reaches the background sensitivity of the SIMS tool by 500 °C annealing. A portion of this lower concentration population is likely to be F^- that compensates the Si donors through the reaction $F^- + Si^+ \leftrightarrow$ F-Si. This was first observed in AlInAs, where a correlation between fluorine accumulation and Si donor concentration in intrinsic or n-type AlInAs layers was only observed in the former.[3,4] The experimental results in that case were explained by two different populations of F, namely immobile F bound to a Si donor, and in the other, it is freely diffusing neutral form.[4] It is still to be established whether the association of the fluorine with the Si donors is simply compensation, where the electron mobility would decrease, or a passivation reaction, where a neutral complex would form and the electron mobility in that region would increase due to reduced carrier scattering. The previous theory[27] suggests that under some conditions, F and Cl are shallow donors that may contribute to the n-type conductivity of Ga_2O_3. What we see under our conditions of post-growth incorporation is that the F is a compensator of donors.

In the FLOOPS simulations, we assumed that the outdiffusion of the large, near-surface concentration was mediated through fluorine molecule formation. Even though the plasma exposure itself created defects that altered the barrier height, these are annealed out before the bulk of the fluorine begins to outdiffuse. The dominant reaction is now $F^0 + F^0 \leftrightarrow F_2$. The overall reaction rate is given by $R_C = K_{for}[F]^2 - K_{rev}[F_2]$, where K_{for} is the forward reaction rate and K_{rev} is the reverse reaction rate. The fluorine diffusion-reaction equations are given by

$$\frac{d^2F}{dt} - DF\frac{dF}{dx} + Rc = 0$$

$$\frac{dF}{dt} - Rc = 0,$$

where F and F_2 are the fluorine and fluorine molecule concentrations, respectively. Neumann boundary conditions at the Ga_2O_3 surface were implemented that represent F_2

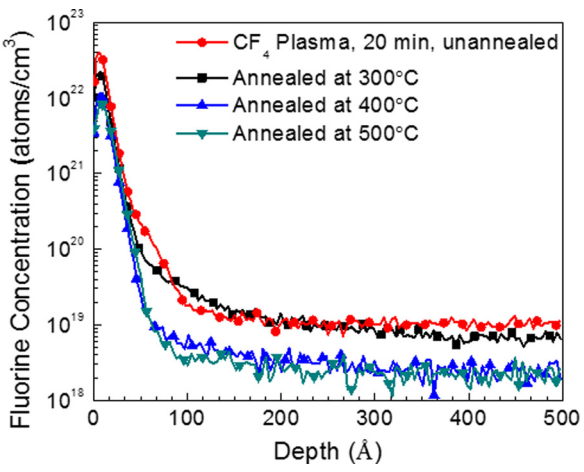

FIG. 7. SIMS profiles of F in Ga_2O_3 exposed to CF_4 plasmas for 20 min and then subsequently annealed in the range 300–500 °C.

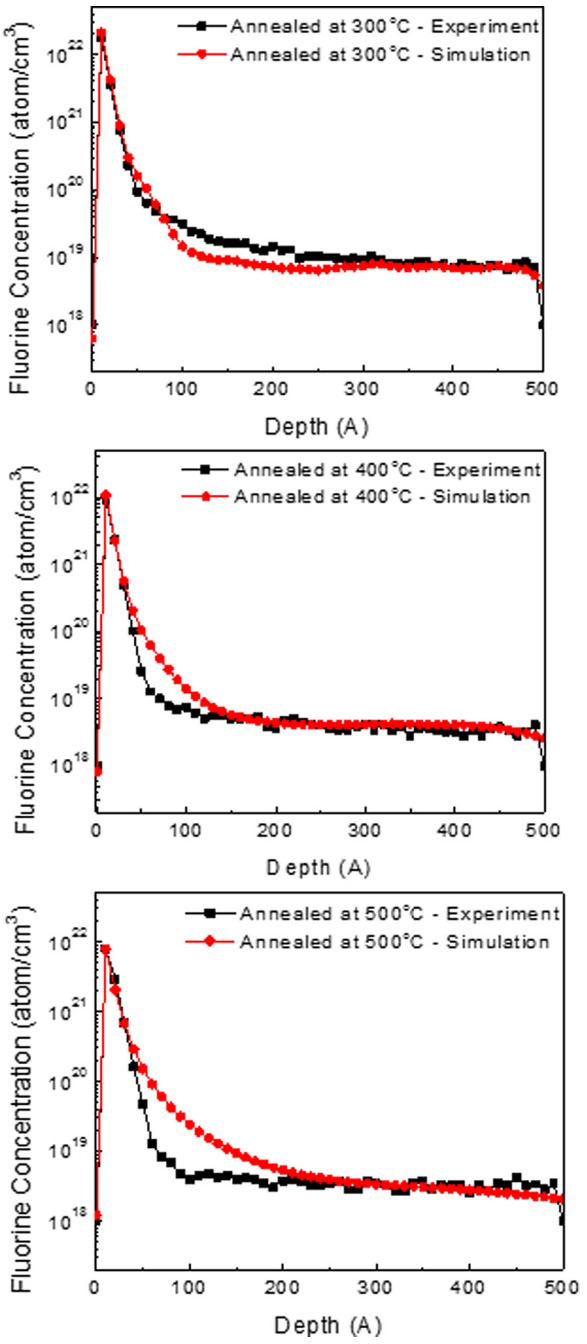

FIG. 8. Experimental and simulated fluorine profiles at different annealing temperatures (300 °C, top, 400 °C, center, and 500 °C, bottom), from which we extracted the values for activation energy of diffusion and outgassing.

outgassing with flux equal to: $K_S \times F$, where K_S is the surface outgas rate of F and was tuned to fit the experimental data. Examples of the fitted data are shown in Fig. 8 for the samples annealed at 300, 400, and 500 °C. The activation energy for diffusion was obtained by fitting the experimental data at the different annealing temperatures, as shown in Fig. 9 (top), with a value of 1.23 eV. The forward and reverse reaction rates, K_{for}, K_{rev}, were also tuned to fit the data and followed Arrhenius dependence with temperature, as shown in Fig. 9 (bottom). The respective values of these parameters were 1.24 and 0.34 eV, respectively.

The simulation results of the amount of fluorine remaining at each annealing temperature, shown in Fig. 10, provide a slightly skewed fit to the F retention data at each annealing temperature, which is by the likely presence of re-trapping, but provides a good estimate of the activation energy needed for outgassing of the high near-surface fluorine, 1.24 eV. This is quite similar to the value reported for outgassing of deuterium,[40] another mobile electrically active impurity in Ga_2O_3. The activation energy of fluorine diffusion and the thermal activation energy of the surface outgas rate are in principle the same. It is possible that the latter is smaller than the diffusion activation energy and that the outgas rate is determined by the diffusion process.

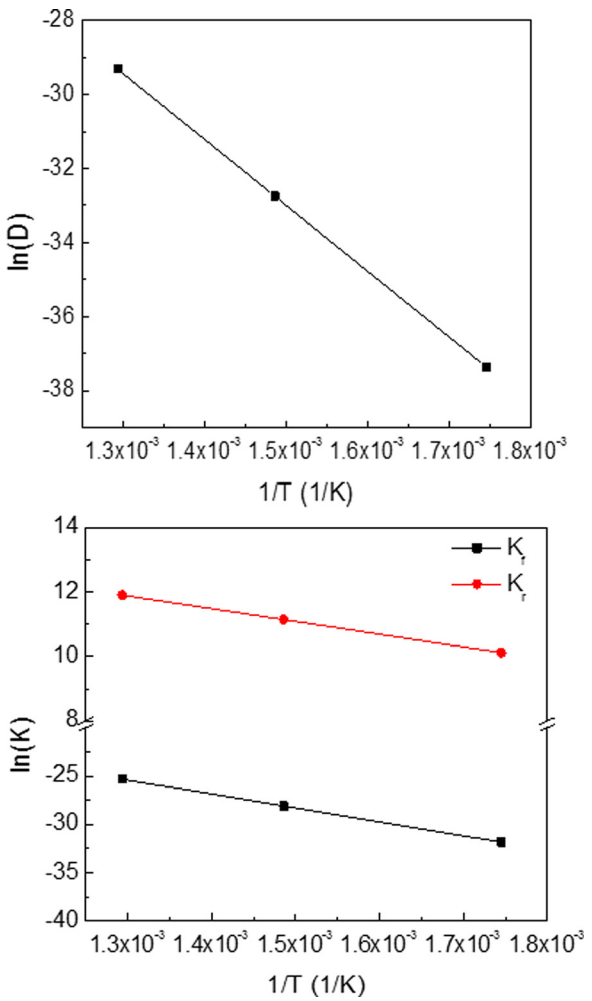

FIG. 9. Arrhenius plots of diffusivity (top) and forward and reverse reaction rates (bottom).

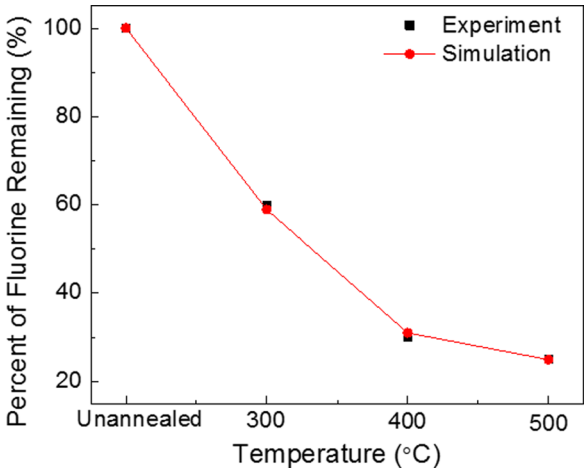

FIG. 10. Percentage of F remaining in Ga_2O_3 after exposure to CF_4 plasmas for 20 min and then subsequent annealing in the range 300–500 °C, along with the values simulated by FLOOPS.

SUMMARY AND CONCLUSIONS

Fluorine is found to be incorporated at high concentrations into Ga_2O_3 and is present in at least two forms. These are a fairly immobile, high concentration form that is likely to be molecules and the other is atomic fluorine that can be ionized to compensate Si donors. There is an initial barrier height lowering, which is due to ion bombardment damage, but once this is annealed out, the Schottky barrier heights are higher than the reference sample for annealing above 300 °C due to the chemical influence of the fluorine. The experimental data were accurately fit by a process simulator, allowing extraction of activation energies for diffusion, outgassing, and forward and reverse fluorine molecule reaction rates.

ACKNOWLEDGMENTS

The project was sponsored by the Department of the Defense, Defense Threat Reduction Agency, HDTRA1-17-1-011, monitored by Jacob Calkins. The content of the information does not necessarily reflect the position or the policy of the federal government, and no official endorsement should be inferred. Part of the work at Tamura was supported by "The research and development project for innovation technique of energy conservation" of the New Energy and Industrial Technology Development Organization (NEDO), Japan. We also thank Dr. Kohei Sasaki from Tamura Corporation for fruitful discussions.

[1]A. Wakejima, K. Onda, Y. Ando, A. Fujihara, E. Mizuki, T. Nakayama, H. Miyamoto, and M. Kuzuhara, J. Appl. Phys. **81**, 1311 (1997).
[2]N. Hayafuji, Y. Yamamoto, N. Yoshida, T. Sonoda, S. Takamiya, and S. Mitsui, Appl. Phys. Lett. **66**, 863 (1995).
[3]N. Hayafuji, Y. Yamamoto, T. Ishida, and K. Sato, Appl. Phys. Lett. **69**, 4075 (1996).
[4]A. Wakejima, K. Onda, A. Fujihara, E. Mizuki, and M. Kanamori, Appl. Phys. Lett. **73**, 2459 (1998).
[5]Y. Cai, Y. G. Zhou, K. J. Chen, and K. M. Lau, IEEE Electron Device Lett. **26**, 435 (2005).
[6]Y. Cai, Y. Zhou, K. M. Lau, and K. J. Chen, IEEE Trans Electron Devices **53**, 2207 (2006).
[7]T. Palacios, C.-S. Suh, A. Chakraborty, S. Keller, S. P. DenBaars, and U. K. Mishra, IEEE Electron Device Lett. **27**, 428 (2006).

[8]H. Mizuno, S. Kishimoto, K. Maezawa, and T. Mizutani, Phys. Status Solidi C **4**, 2732 (2007).
[9]K. Konishi, K. Goto, H. Murakami, Y. Kumagai, A. Kuramata, S. Yamakoshi, and M. Higashiwaki, Appl. Phys. Lett. **110**, 103506 (2017).
[10]A. Kuramata, K. Koshi, S. Watanabe, Y. Yamaoka, T. Masui, and S. Yamakoshi, Jpn. J. Appl. Phys., Part 1 **55**, 1202A2 (2016).
[11]H. Von Wenckstern, Adv. Electron. Mater. **3**, 1600350 (2017).
[12]M. Baldini, M. Albrecht, A. Fiedler, K. Irmscher, R. Schewski, and G. Wagner, ECS J. Solid State Sci. Technol. **6**, Q3040 (2017).
[13]S. J. Pearton, J. Yang, P. H. Cary IV, F. Ren, J. Kim, M. J. Tadjer, and M. A. Mastro, Appl. Phys. Rev. **5**, 011301 (2018).
[14]A. Pérez-Tomás, E. Chikoidze, M. R. Jennings, S. A. O. Russell, F. H. Teherani, P. Bove, E. V. Sandana, and D. J. Rogers, Proc. SPIE **10533**, 105331Q (2018).
[15]D. Gogova, G. Wagner, M. Baldini, M. Schmidbauer, K. Irmscher, R. Schewski, Z. Galazka, M. Albrecht, and R. Fornari, J. Cryst. Growth **401**, 665 (2014).
[16]R. Fornari, M. Pavesi, V. Montedoro, D. Klimm, F. Mezzadri, I. Cora, B. Pécz, F. Boschi, A. Parisini, A. Baraldi, C. Ferrari, E. Gombia, and M. Bosi, Acta Mater. **140**, 411 (2017).
[17]E. Farzana, Z. Zhang, P. K. Paul, A. R. Arehart, and S. A. Ringel, Appl. Phys. Lett. **110**, 202102 (2017).
[18]Y. Yao, R. Gangireddy, J. Kim, K. K. Das, R. F. Davis, and L. M. Porter, J. Vac. Sci. Technol. B **35**, 03D113 (2017).
[19]Z. Galazka, R. Uecker, D. Klimm, K. Irmscher, M. Naumann, M. Pietsch, A. Kwasniewski, R. Bertram, S. Ganschow, and M. Bickermann, ECS J. Solid State Sci. Technol. **6**, Q3007 (2017).
[20]M. Higashiwaki, K. Sasaki, H. Murakami, Y. Kumagai, A. Koukitu, A. Kuramata, T. Masui, and S. Yamakosh, Semicond. Sci. Technol. **31**, 034001 (2016).
[21]H. Y. Playford, A. C. Hannon, E. R. Barney, and R. I. Walton, Chem. - Eur. J. **19**, 2803 (2013).
[22]M. Higashiwaki and G. H. Jessen, Appl. Phys. Lett. **112**, 060401 (2018).
[23]M. J. Tadjer, M. A. Mastro, N. A. Mahadik, M. Currie, V. D. Wheeler, J. A. Freitas, J. D. Greenlee, J. K. Hite, K. D. Hobart, C. R. Eddy, and F. J. Kub, J. Electron. Mater. **45**, 2031 (2016).
[24]S. Rafique, L. Han, and H. Zhao, ECS Trans. **80**, 203 (2017).
[25]M. Higashiwaki, A. Kuramata, H. Murakami, and Y. Kumagai, J. Phys. D: Appl. Phys. **50**, 333002 (2017).
[26]M. A. Mastro, A. Kuramata, J. Calkins, J. Kim, F. Ren, and S. J. Pearton, ECS J. Solid State Sci. Technol. **6**, P356 (2017).
[27]J. B. Varley, J. R. Weber, A. Janotti, and C. G. Van de Walle, Appl. Phys. Lett. **97**, 142106 (2010).
[28]W. B. Fowler, P. Weiser, and M. Stavola, APS March Meeting Abstracts, 2017.
[29]D. Gogova, M. Schmidbauer, and A. Kwasniewski, Cryst. Eng. Commun. **17**, 6744 (2015).
[30]J. E. Hogan, S. W. Kaun, E. Ahmadi, Y. Oshima, and J. S. Speck, Semicond. Sci. Technol. **31**, 065006 (2016).
[31]A. P. Shah and A. Bhattacharya, J. Vac. Sci. Technol. A **35**, 041301 (2017).
[32]J. Yang, S. Ahn, F. Ren, S. J. Pearton, R. Khanna, K. Bevlin, D. Geerpuram, and A. Kuramata, J. Vac. Sci. Technol. B **35**, 031205 (2017).
[33]J. Yang, F. Ren, R. Khanna, K. Bevlin, D. Geerpuram, L.-C. Tung, J. Lin, H. Jiang, J. Lee, E. Flitsiyan, L. Chernyak, S. J. Pearton, and A. Kuramata, J. Vac. Sci. Technol. B **35**, 051201 (2017).
[34]G. Yang, S. Jang, F. Ren, S. J. Pearton, and J. Kim, ACS Appl. Mater. Interfaces **9**, 40471 (2017).
[35]J. Yang, Z. Chen, F. Ren, S. J. Pearton, G. Yang, J. Kim, J. Lee, E. Flitsiyan, L. Chernyak, and A. Kuramata, J. Vac. Sci. Technol. B **36**, 011206 (2018).
[36]See https://www.eag.com for EAG Laboratories.
[37]See http://www.tec.ufl.edu/~flooxs/FLOOXS%20Manual/Intro.html for information about the coding,materials databases and applications.
[38]M. E. Law and S. Cea, Comput. Mater. Sci. **12**, 289 (1998).
[39]E. Patrick, M. Choudhury, F. Ren, S. J. Pearton, and M. Law, ECS J. Solid State Sci. Technol. **4**, Q21 (2015).
[40]R. Sharma, E. Patrick, M. E. Law, S. Ahn, F. Ren, S. J. Pearton, and A. Kuramata, ECS J. Solid State Sci. Technol. **6**, P794 (2017).
[41]S. Ringel, E. Farzana, J. McGlone, Z. Xia, Y. Zhang, C. Joishi, E. Ahmadi, A. Mauze, T. Blue, S. Rajan, J. S. Speck, and A. Arehart, "The presence and impact of deep level defects induced by high energy neutron radiation in beta-phase gallium oxide," paper presented at GOMAC 2018, Miami, FL, March 2018.